

Tuning magnetic properties of Mn₄ cluster with gold coating

Q. Wang,^{*ab} Q. Sun,^{cb} P. Jena^b and Y. Kawazoe^d

Received 8th October 2009, Accepted 25th November 2009

First published as an Advance Article on the web 5th January 2010

DOI: 10.1039/b921095d

The magnetic properties of transition metal clusters are a unique function of their size and differ from their bulk behavior due to quantum confinement. Here we show that surface modification provides another channel to tune their magnetic properties. This is demonstrated by taking Mn₄ as an example. Although Mn₄ carries a giant magnetic moment of 20 μ_B , the magnetic coupling can be tuned from ferromagnetic to ferrimagnetic by changing the number of gold atoms coated on its surface. We found that 26 gold atoms are needed to fully cover a Mn₄ cluster. When partially coated, the system exhibits ferromagnetic coupling with a total magnetic moment of 18 μ_B and it becomes ferrimagnetic with a moment of 8 μ_B when fully coated. This magnetic cross-over is caused by the shrinking of the Mn–Mn bond length, suggesting that the magnetic properties of a Mn₄ cluster can be tuned by controlling the surface coverage.

Introduction

The properties of transition metals are governed primarily by their unfilled d orbitals which are localized as compared to simple metals where the s and p electrons are delocalized. Thus, the geometry, relative stability, and electronic structure of transition metal clusters do not follow any simple rule. Due to their rich magnetic properties, transition metal clusters have important applications in many fields including magnetic recording, catalysis, biomedical science, *etc.* As a matter of fact, considerable efforts have currently been devoted to explore the application of transition metal nanostructures in magnetic resonance imaging contrast enhancement, tissue repair, immunoassays, detoxification of biological fluid, hyperthermia, targeted drug delivery and cell separation.^{1–7} Since nano-particles have the same length scales as those of tumors, they can provide some attractive possibilities to treat malignant tumors, where the strategy is to implant a nanoparticle near a cancer cell that can be heated through near infrared (NIR) light or an alternating magnetic field, and the resulting heat can then destroy the tumor cells without damaging the healthy tissues. In practice, besides being small in size, a very basic requirement of the nano-particles is that they have a high magnetic moment. For this reason, magnetic clusters are attractive since their magnetic moment can be enhanced due to reduced coordination and dimensionality.

Among the transition metal clusters, Mn₄ is of interest. A Mn atom, due to its half filled 3d and filled 4s shells (3d⁵4s²), interacts weakly and bulk Mn has the lowest cohesive energy of any 3d transition metal system. The magnetic moment of

Mn atom is 5 μ_B and small clusters of Mn containing 3 to 5 atoms couple ferromagnetically while bulk Mn is anti-ferromagnetic. Mn₄ carries a giant magnetic moment of 20 μ_B ⁸ which is retained even when it is embedded in a rare gas matrix.⁹ However, the bare Mn clusters cannot directly be used for bio-applications, because they are not biocompatible and not chemical stable, they can easily be oxidized. Therefore, these clusters need to be functionalized. Gold has been recognized as the best candidate for coating due to its bio-compatibility, functionality with various enzymes, chemical inertness, and flexible geometries.^{10–16} It is therefore of interest to study how gold coating affects the magnetic properties of Mn₄ cluster. For example: (1) How many Au atoms are needed to fully coat a Mn₄ cluster? (2) How does Au coating change the magnetic properties of a Mn₄ cluster? Can the giant magnetic moment be retained after gold coating? (3) How do the resulting changes depend on the number of coated gold atoms? In this paper, using density functional theory we have systematically studied the geometry, electronic structure and magnetic properties of Mn₄ cluster coated with increasing number of Au atoms, Mn₄@Au_{*n*} (*n* = 8, 14, 20, 26 and 32). We have found that the system displays complicated magnetic behavior when more gold atoms are added. This suggests that the magnetic properties of Mn clusters can be tuned by surface modification.

Computational method

The calculations were carried out using density functional theory and generalized gradient approximation (GGA) for exchange and correlation with PW91 functional,¹⁷ which is better than LDA for magnetism.¹⁸ We used plane wave basis set with the projector augmented wave (PAW) method¹⁹ with the valence states 5d¹⁰6s¹ for Au and 3p⁶3d⁵4s² for Mn, as implemented in the Vienna *ab initio* simulation package (VASP).²⁰ We used a supercell approach where Mn₄@Au₃₂ and Mn₄@Au₂₆ clusters were placed at the center of a 24 × 24 × 24 Å³ cubic cell, while the electronic structure and magnetic properties of Mn₄@Au₂₀, Mn₄@Au₁₄, and Mn₄@Au₈ were

^a School of Physical Science and Technology, Southwest University, Chongqing 400715, China. E-mail: qwang@vcu.edu

^b Physics Department, Virginia Commonwealth University, Richmond, VA 23284

^c Department of Advanced Materials and Nanotechnology, and Center for Applied Physics and Technology, Peking University, Beijing 1000871, China

^d Institute for Materials Research, Tohoku University, Sendai, 980-8577, Japan

calculated using $22 \times 22 \times 22$, $21 \times 21 \times 21$ and $20 \times 20 \times 20 \text{ \AA}^3$ supercells, respectively. The geometries were optimized without any symmetry constraint and high precision calculations with a cutoff energy of 450 eV for the plane-wave basis were performed. The total energies, electronic structure, and magnetic moments on each Mn atom were calculated self-consistently for each possible spin multiplicity ranging from 1 to 21. In all calculations, self-consistency was achieved with a tolerance in the total energy of at least 0.3 meV. Hellman–Feynman force components on each ion in the supercells were converged to 3 meV \AA^{-1} .

Results and conclusions

In Fig. 1 we provide the starting geometries and the corresponding optimized structures of $\text{Mn}_4@Au_n$ ($n = 8, 14, 20, 26$ and 32) clusters. Note Mn_4 has T_d symmetry and carries a giant magnetic moment of $20 \mu_B$. This lowest energy spin configuration is 0.117 eV lower in energy than the next stable spin state of $10 \mu_B$. The change of the relative energies, calculated with respect to the lowest energy spin configuration of $20 \mu_B$, is plotted in Fig. 2(a) for all the possible spin states. Its equilibrium Mn–Mn bond length is 2.717 \AA . In order to cover the Mn_4 cluster with Au, we first introduced eight Au atoms, four of them are capped on the triangle surfaces, and the other four are on the top site of Mn atoms, resulting in an initial geometry of $\text{Mn}_4@Au_8$ with T_d symmetry, as shown in Fig. 1(a₁). The geometry optimization and a detailed calculation for different spin multiplicities ranging from 1 to 21 were carried out. It is found that the lowest energy state with a total magnetic moment of $18 \mu_B$ is 0.202 eV lower in energy than the spin state with a magnetic moment of $20 \mu_B$, 0.105 eV lower than the state with a moment of $10 \mu_B$, and 0.644 eV lower than the antiferromagnetic state (total spin = $0 \mu_B$) [see Fig. 2(b)]. In the lowest energy spin state, the geometry is totally different from the initial one and the symmetry changes to C_2 from T_d [see Fig. 1(a₂)]. The smallest Mn–Mn bond length is 2.973 \AA and the average Au–Mn bond length is 2.641 \AA . The total magnetic moment of $\text{Mn}_4@Au_8$ reduces to $18 \mu_B$ (compared to $20 \mu_B$ of Mn_4) due to the hybridization of atomic orbitals of Mn and the coated Au atoms. The local moment on each Mn atom is about $4.00 \mu_B$ and mainly comes from Mn 3d orbitals ($3.94 \mu_B$) with small contribution from Mn 3p and 4s. The Au atoms are polarized ferromagnetically with an average magnetic moment of $0.08 \mu_B/Au$. The calculated spin density distribution is plotted in Fig. 3(a), which clearly shows the ferromagnetic coupling between the Mn atoms and the ferromagnetic polarization of Au atoms in the $\text{Mn}_4@Au_8$ cluster. The gold atoms prefer to be close to each other and leave the Mn sites partially uncovered [see Fig. 1(a₂)], indicating that eight Au atoms are not enough for completely coating the Mn_4 cluster.

We then introduced six more Au atoms to $\text{Mn}_4@Au_8$ by placing one Au atom in the center of each Au–Au edge, generating the $\text{Mn}_4@Au_{14}$ cluster with T_d symmetry as shown in Fig. 1(b₁). The initial geometry changes to C_1 symmetry after optimization. The lowest energy spin state still carries a total magnetic moment of $18 \mu_B$, which is lower in energy by 0.122 to 1.324 eV than other spin states. For example, the spin

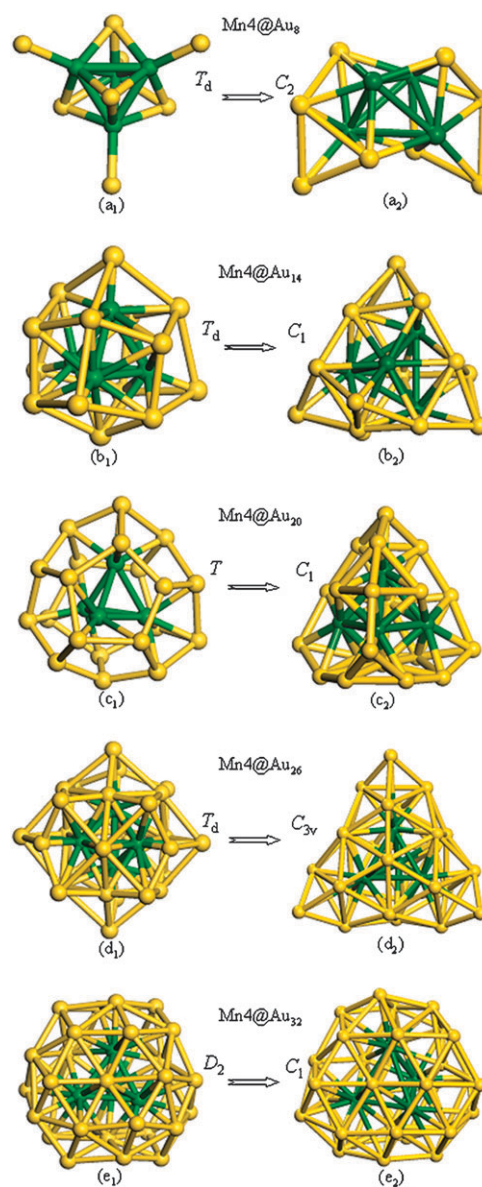


Fig. 1 (a₁), (b₁), (c₁), (d₁), and (e₁) represent starting structures of the five Au-coated Mn_4 clusters. Optimized geometries and their corresponding symmetries are given in (a₂), (b₂), (c₂), (d₂), and (e₂), respectively.

state with a total magnetic moment of $20 \mu_B$ becomes 1.11 eV higher in energy than that of $18 \mu_B$ configuration. The calculated results are given in Fig. 2(c) and Table 1. We note that the Mn–Mn and the Au–Mn bond lengths are slightly enlarged compared to those in the $\text{Mn}_4@Au_8$ cluster, but Mn atoms are still partially exposed, suggesting even more Au atoms are needed to completely cover the Mn_4 cluster.

Next, we considered an $\text{Mn}_4@Au_{20}$ cluster that has six more Au atoms than the previous case. The initial geometry has T symmetry [Fig. 1(c₁)], which changed to C_1 symmetry after geometry optimization. It is interesting to see that the skeleton of the coated Au atoms is similar to that of Au_{20} . The spin states with a total magnetic moment of $16 \mu_B$ and $18 \mu_B$ are energetically degenerate with the former lying about 0.024 eV

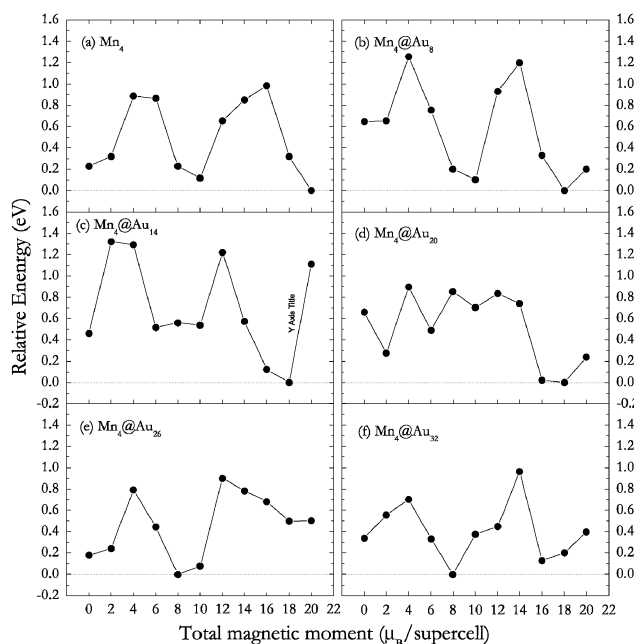


Fig. 2 Relative energies of different magnetic configurations of (a) Mn_4 , (b) $\text{Mn}_4@Au_8$, (c) $\text{Mn}_4@Au_{14}$, (d) $\text{Mn}_4@Au_{20}$, (e) $\text{Mn}_4@Au_{26}$ and $\text{Mn}_4@Au_{32}$ clusters measured with respect to their respective lowest energy spin configuration.

higher in energy than the latter one. The other spin states are higher in energy by 0.239 to 0.898 eV than ones above. Fig. 2(d) shows that the change of relative energy with spin multiplicity has an oscillating behavior. However, the Mn_4 cluster is still not fully covered by the Au atoms.

To fully coat the Mn_4 cluster, we further studied $\text{Mn}_4@Au_{26}$. We started with an initial geometry having T_d symmetry, which becomes C_{3v} after optimization [see Fig. 1(d₁) and (d₂)]. Now all the Mn atoms in Mn_4 cluster are completely coated. The total magnetic moment in the lowest energy state, however, is reduced to $8 \mu_B$, where one Mn atom becomes antiferromagnetically coupled with the others, carrying a magnetic moment of $-3.874 \mu_B$. This ferrimagnetic state of $\text{Mn}_4@Au_{26}$ is 0.496 and 0.501 eV lower in energy than the ferromagnetic states with total magnetic moments of 18 and $20 \mu_B$, respectively [see Fig. 2(e)]. The neighboring Au atoms of Mn are polarized in the same spin direction as the nearing Mn atoms with an average magnetic moment of -0.006 and $0.038 \mu_B/Au$, respectively. The minimal Mn–Mn bond length of the antiferromagnetically coupled

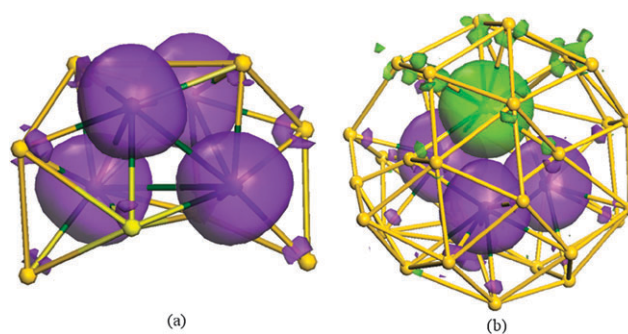


Fig. 3 Spin density isosurface at the isovalue of $0.22 e \text{ \AA}^{-3}$ for the ferromagnetic $\text{Mn}_4@Au_8$ (a) and the ferrimagnetic $\text{Mn}_4@Au_{32}$ (b). The purple is for spin-up and the green is for spin-down states.

Mn pairs is 2.701 \AA , which is significantly shorter than the corresponding values in the $\text{Mn}_4@Au_n$ ($n = 8, 14, 20$) clusters.

To see if the ferrimagnetic coupling of fully gold coated Mn_4 cluster can reverse to ferromagnetic behavior if further gold atoms are added to the surface we generated a $\text{Mn}_4@Au_{32}$ cluster with D_2 symmetry by embedding the Mn_4 cluster into the center of an Au_{32} cage [see Fig. 1(e₁)]. The optimized structure becomes C_1 symmetry with a total magnetic moment of $8 \mu_B$, which is 0.128 to 0.964 eV lower in energy than other spin states [see Fig. 2(f)]. In this lowest energy spin state, we found, once again, that the cluster is ferrimagnetic with one Mn atom coupled antiferromagnetically with the other three Mn atoms, while the three Mn atoms coupled ferromagnetically to each other. The neighboring Au atoms of Mn are weakly polarized carrying a moment of 0.011 and $-0.022 \mu_B$, accordingly, which is visualized by the spin density distributions in Fig. 3(b). We noted that although $\text{Mn}_4@Au_{26}$ and $\text{Mn}_4@Au_{32}$ are different in size and geometry they share the common magnetic properties; they are both ferrimagnetic with a total magnetic moment of $8 \mu_B$.

The main results of our calculations are summarized in Table 1, from which the following conclusions can be drawn: (1) As more Au atoms are coated to the Mn_4 surface, the HOMO–LUMO gap decreases. (2) In the partially coated $\text{Mn}_4@Au_n$ ($n = 8, 14, 20$) clusters the Mn–Mn bond length is elongated and the ferromagnetic coupling between Mn atoms is retained, as compared to those of the uncoated Mn_4 cluster. When fully coated the Mn–Mn bond length in $\text{Mn}_4@Au_n$ ($n = 26, 32$) clusters shrink, and the magnetic coupling becomes ferrimagnetic. It has been established that the magnetic couplings between Mn atoms are sensitive

Table 1 The HOMO–LUMO gaps Δ_{gap} (in eV), the minimal Mn–Mn bond length $d_{\text{Mn–Mn}}$ and the average Au–Mn bond lengths $d_{\text{Au–Mn}}$ (in \AA), the total magnetic moment M_{total} and the local magnetic moment M_i (in μ_B) on each Mn atom, and the induced moment on Au atoms (in μ_B/Au) for the lowest energy magnetic configuration of each cluster given in Fig. 1

Clusters	Δ_{gap}	$d_{\text{Mn–Mn}}$	$d_{\text{Au–Mn}}$	M_{total}	M_1	M_2	M_3	M_4	M_{Au}
Mn_4	0.574	2.717	—	20	5.0	5.0	5.0	5.0	—
$\text{Mn}_4@Au_8$	0.309	2.973	2.641	18	3.996	4.025	3.996	4.024	0.080
$\text{Mn}_4@Au_{14}$	0.256	3.034	2.687	18	4.012	3.991	3.990	3.990	0.056
$\text{Mn}_4@Au_{20}$	0.140	3.310	2.685	18	4.001	4.014	3.998	4.013	0.052
$\text{Mn}_4@Au_{26}$	0.138	2.701	2.687	8	3.802	-3.874	3.702	3.804	0.038–0.006
$\text{Mn}_4@Au_{32}$	0.129	2.710	2.701	8	4.038	-4.016	3.996	3.954	0.011–0.022

to their distance.^{21–23} For example, in orthorhombic and monoclinic-layered LiMnO₂, when the Mn–Mn distance changes from 2.82 to 2.79 Å, the coupling changes from the ferromagnetic phase to the antiferromagnetic phase.²¹ Theoretically, Hobbs and co-workers²² studied the distance dependence of the exchange pair-interactions in a Heisenberg-like model for bulk Mn, and they found that antiferromagnetic coupling is favored at short interatomic distances, which switches to ferromagnetic coupling at larger bond lengths. It is this sensitivity of magnetic coupling to the Mn–Mn bond distance that makes Mn bulk displaying very complicated magnetic structures ranging from nonmagnetic, to antiferromagnetic, low spin ferrimagnetic, and high spin ferromagnetic phases.^{22,23} Here we have shown that surface coating provides another way to achieve the same purpose, namely tune the magnetic coupling in Mn clusters by changing the bond length. (3) Mn atom polarizes ferromagnetically its neighboring Au atoms. In the partially coated clusters, due to the ferromagnetic coupling among Mn atoms, all the polarized Au atoms have the same spin orientation, while for the fully coated ones, the ferrimagnetically coupled Mn atoms also induce the moments on Au atoms, but with different spin orientations due to the ferromagnetic polarization of Au atoms. (4) We note that full coating can easily result in ferrimagnetism in Mn₄@Au_n clusters, and their total magnetic moments are reduced considerably.

Acknowledgements

This work is partially supported by grants from the National Natural Science Foundation of China (10874007), the US National Science Foundation, and the US Department of Energy. The authors thank the staff of the Center for Computational Materials Science, the Institute for Materials Research, Tohoku University (Japan), for their continuous support of the HITACH SR11000 supercomputing facility.

References

- 1 T. Matsunaga, Y. Okamura and T. Tanaka, *J. Mater. Chem.*, 2004, **14**, 2099.
- 2 S. Bucak, D. A. Jones, P. E. Laibinis and T. A. Hatton, *Biotechnol. Prog.*, 2003, **19**, 477.
- 3 M. Koneracka, P. Kopcansky, M. Timko and C. N. Ramchand, *J. Magn. Magn. Mater.*, 2002, **252**, 409.
- 4 Z. G. Forbes, B. B. Yellen, K. A. Barbee and G. Friedman, *IEEE Trans. Magn.*, 2003, **39**, 3372.
- 5 P. Tartaj, M. Morales, S. V. Verdaguier, T. G. Carreño and C. J. Serna, *J. Phys. D: Appl. Phys.*, 2003, **36**, R182.
- 6 Q. A. Pankhurst, J. Connolly, S. K. Jones and J. Dobson, *J. Phys. D: Appl. Phys.*, 2003, **36**, R167.
- 7 S. Mornet, S. Vasseur, F. Grasset and E. Duguet, *J. Mater. Chem.*, 2004, **14**, 2161.
- 8 S. K. Nayak, B. K. Rao and P. Jena, *J. Phys.: Condens. Matter*, 1998, **10**, 10863.
- 9 C. A. Baumann, R. J. VanZee, S. Bhat and W. Weltner Jr., *J. Chem. Phys.*, 1983, **78**, 190.
- 10 R. F. Service, *Nature*, 2004, **306**, 2035.
- 11 Q. Sun, Q. Wang, B. K. Rao and P. Jena, *Phys. Rev. Lett.*, 2004, **93**, 186803.
- 12 J. Aizpurua, P. Hanarp, D. S. Sutherland, M. Käll, G. W. Bryant and F. J. García-de-Abramo, *Phys. Rev. Lett.*, 2003, **90**, 57401.
- 13 Q. Sun, A. K. Kandalam, Q. Wang, P. Jena, Y. Kawazoe and M. Marquez, *Phys. Rev. B: Condens. Matter Mater. Phys.*, 2006, **73**, 134409.
- 14 Q. Sun, B. V. Reddy, M. Marquez, P. Jena, C. Gonzalez and Q. Wang, *J. Phys. Chem. C*, 2007, **111**, 4159.
- 15 M. P. Johansson, D. Sundholm and J. Vaara, *Angew. Chem., Int. Ed.*, 2004, **43**, 2678.
- 16 Y. Kondo and K. Takayanagi, *Science*, 2000, **289**, 606.
- 17 Y. Wang and J. P. Perdew, *Phys. Rev. B: Condens. Matter*, 1991, **44**, 13298.
- 18 T. C. Leung, C. T. Chan and B. N. Harmon, *Phys. Rev. B: Condens. Matter*, 1991, **44**, 2923.
- 19 G. Kresse and J. Joubert, *Phys. Rev. B: Condens. Matter Mater. Phys.*, 1999, **59**, 1758.
- 20 G. Kresse and J. Furthmüller, *Phys. Rev. B: Condens. Matter*, 1996, **54**, 11169.
- 21 G. Ceder and S. K. Mishra, *Electrochem. Solid-State Lett.*, 1999, **2**, 550.
- 22 D. Hobbs, J. Hafner and D. Spisak, *Phys. Rev. B: Condens. Matter Mater. Phys.*, 2003, **68**, 014407.
- 23 J. Hafner and D. Hobbs, *Phys. Rev. B: Condens. Matter Mater. Phys.*, 2003, **68**, 014408.